PAPER • **OPEN ACCESS**

Finite element modelling of indentation testing in an AA1050 microstructure

To cite this article: S Goutianos *et al* 2022 *IOP Conf. Ser.: Mater. Sci. Eng.* **1249** 012031

Finite element modelling of indentation testing in an AA1050 microstructure

S Goutianos[1], H Pan[2,3] and X Zhang[2]

[1] Department of Manufacturing and Civil Engineering, Norwegian University of Science and Technology, 2815 Gjøvik, Norway
[2] Department of Mechanical Engineering, Technical University of Denmark, Kongens Lyngby, 2800, Denmark
[3] Department of Materials Science and Engineering, Kunming University of Science and Technology, Kunming 650093, China

E-mail: stergios.goutianos@ntnu.no

Abstract. Heterogeneous microstructures can be produced in structural metals from heterogeneous deformation, and they can also be purposely designed to meet specific requirements in high-demanding engineering applications. When designing a heterogeneous microstructure in metallic materials, it is important to know the local mechanical properties such as the stress-strain behavior. However, due to the local varying microstructure, direct measurement of the local mechanical properties is not feasible either by bulk testing or by miniature testing. In this work, an iterative approach, based on the finite element method and under the assumption that the local mictrostructure is homogeneous, will be presented as an example to extract the local mechanical properties of cold-rolled AA1050 from indentation tests as an example. The uncertainties of the proposed method are discussed.

1. Introduction

Plastic deformation of metals typically refines the microstructure and results in high strength [1]. Several approaches have been developed to introduce high strains in bulk samples in order to obtain high strength metals. Alternatively, an increased strength can be also obtained by limiting the hard nanostructure only close to the surface region e.g. by shot-peening [1, 2, 3]. In this case, the resultant microstructure is not homogeneous. Similarly, graded microstructures can be generated in the surface and its neighboring region by surface deformation such as friction and wear [4, 5]. In both cases, the microstructures extend only few micrometers to a few tens of micrometers into the bulk material [5, 6], and therefore it is difficult to determine its stress-strain behaviour.

The importance of being able to assess the mechanical properties at such small scales and in parallel the improvements in indentation equipment, have led in a increased interest in instrumented indentation [7]. Several methods have been developed to extract the mechanical properties such as the Young's modulus, E, the yield stress, σ_y and the strain hardening exponent, n, from the indentation load-displacement curves [8, 9]. In general, a reverse analysis, typically using the finite element method, is performed to solve for the three unknowns mentioned above and thus the elasto-plastic material properties can be determined.

The present work follows to a large extend the existing numerical approaches for reverse analysis of indentation experiments. Although, the final aim is to characterize nanostructured graded microstructures, here the numerical method will be illustrated on microstructures in cold-rolled AA1050 (see Fig. 1) and more specifically in 70% cold-rolled AA1050. The present works focuses on the numerical approach, and therefore the experimental details will not be discussed here. However, this method will be incorporated with the experimental methods in near future, to remove the uncertainties in the modelling.

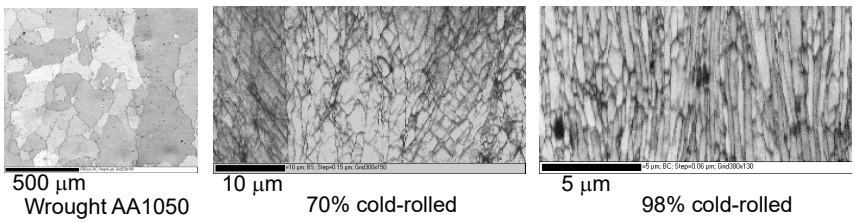

Figure 1. Typical wrought AA1050 microstructure and for 70% and 98% cold-rolling levels.

2. Finite element analysis of micro-indentation

Fig. 2a shows schematically the Berkovich indenter used in the indentation tests. The angle ψ was equal to 65.3^o. A three-dimensional finite element model was built using the finite element program Abaqus. Since a three-dimensional model is computationally expensive even if one sixth of the indenter is modelled due to the three symmetry planes, it is not practical for reverse analysis. Therefore an equivalent axisymmetric finite element model was also built. The equivalent axisymmetric model assumes that the indenter is conical (Fig. 2b) and the angle θ, is given by [10] in order to have the same projected area:

$$\theta = \tan^{-1}\left(\sqrt{\frac{3\sqrt{3}}{\pi}}\tan\psi\right) = 70.3^o \tag{1}$$

A second axisymmetric finite element model with θ equal to ψ [10] was also built. In both the three-dimensional model and the two axisymmetric models, the indenter was assumed to be rigid (modelled as analytical surface). Hard frictional contact was modelled between the indenter and the indented material allowing finite sliding but not interpenetration. The contact accounts for the indenter pile-up or sink-in.

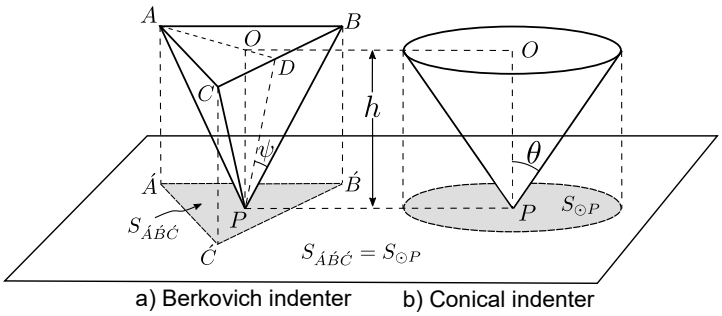

Figure 2. Schematic diagram of the Berkovich indenter with indenter angle ψ, and its equivalent conical indenter with indenter angle θ.

Fig. 3 shows schematically the axisymmetric finite element model with the boundary and loading conditions. The length, L, and the height, H, were large to avoid edge effects. Displacement boundary conditions were applied to reference point (RP), which controls the movement of the indenter in the z-direction during loading and unloading. Since the exact tip geometry of the Berkovich indenter was unknown or difficult to be measured, several tip geometries were modelled: a) tip with sharp edges, and b) tip with a fillet of radius r as shown in Fig. 3. The boundary and loading conditions for the three-dimensional model are analogous and they are not presented here.

A finite element model to simulate and extract the mechanical properties of the bulk cold-rolled aluminum was built (see Section 3.1).

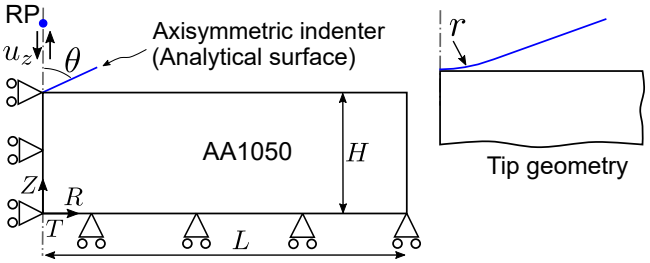

Figure 3. Schematic illustration of the axisymmetric finite element model with boundary and loading conditions.

It was assumed that the indented material can be described by classical isotropic J2 plasticity theory, and that the stress-strain behaviour can be approximated by a power law description:

$$\sigma = \begin{cases} E\varepsilon, & \text{for } \sigma \leq \sigma_y \\ \sigma_o \varepsilon^n, & \text{for } \sigma > \sigma_y \end{cases} \tag{2}$$

3. Results and Discussion

3.1. Tensile stress-strain behaviour

Fig. 4 shows a typical stress-strain curve of 70% cold-rolled AA1050. From the slope of the initial part of the stress-strain curve, the Young's modulus, E, was calculated equal to 63.44 GPa. The tensile experiment was modelled in the Abaqus finite element model assuming that the material follows an elastic-plastic response described by ten points (stress σ, plastic strain ε_{pl}). The first point represents the yield stress, σ_y, of the bulk sample. Then, the Isight optimisation platform was used, in combination with Abaqus, to optimise the modelled elastic-plastic material law. It was found that the yield stress was equal to 79.72 MPa. The elastic modulus and the ten points (σ, ε_{pl}) from the optimisation were used as the starting values in the indentation finite element models e.g. to obtain the initial power law (Eq. 2). This elastic-plastic material law is called here the "reference" material law.

3.2. Indentation response

First, a comparison between the three-dimensional model using a Berkovich indenter and the axisymmetric models (conical indenter) was performed using the "reference" material law (Section 3.1). As can be seen from Fig. 5, when the angle θ is calculated from Eq. 1, the load-displacement curve from axisymmetric model agrees well with the load-displacement curve from the three-dimensional model. As can be seen in Fig. 5 a mesh sensitivity analysis was also performed to increase the confidence in the obtained results.

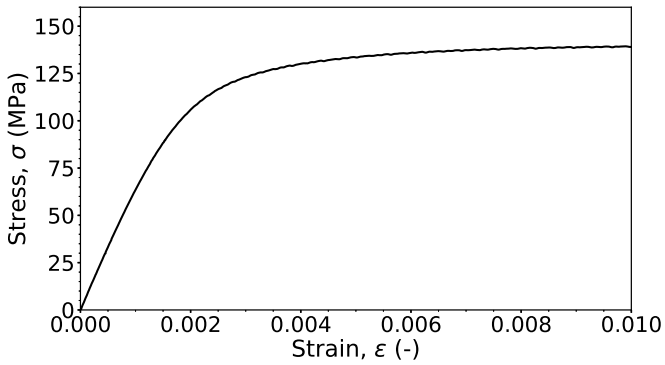

Figure 4. Experimental tensile stress-strain curve of 70% cold-rolled AA1050.

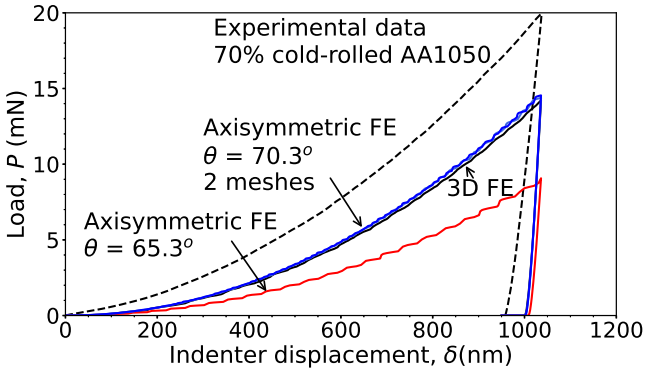

Figure 5. Comparison between 3D finite element (FE) predictions, with a Berkovich indenter, and axisymmetric FE predictions with two different indenter angles θ. The friction coefficient, μ, is equal to 0.1 and the indenter has sharp edges. Fig. 4 was used to extract the elastic-plastic behaviour of AA1050.

It can be seen from Fig. 5 that in all cases, the predicted load-displacement curves, using the "reference" material law, are lower compared to the experimentally obtained load-displacement curve. It should be mentioned that in these simulations the indenters had sharp edges and that the coefficient of friction, μ, was equal to 0.1.

Once it was determined that θ should be equal to 70.3^o, several indentation simulations were performed by varying the elastic-plastic response of the cold-rolled AA1050 in order to have a better agreement with the experimental response. In all cases, it was not possible to match the initial part (for indentation depths approximately up to 200 nm) of the load-displacement curve. A better agreement was found for indenters with rounded tip and as can be seen from Fig. 6. When r is equal to 2 μm the predicted initial part of the load-displacement curve agrees well with the experimental data. It should be mentioned that for larger indentation depths, r should not influence the load-displacement curve.

The effect of the friction coefficient is shown in Fig. 7 for indenters with both sharp and rounded edges. As can be seen the effect of friction is negligible.

Having determined the fillet radius, r, and setting mu equal to 0.1, the elastic-plastic response

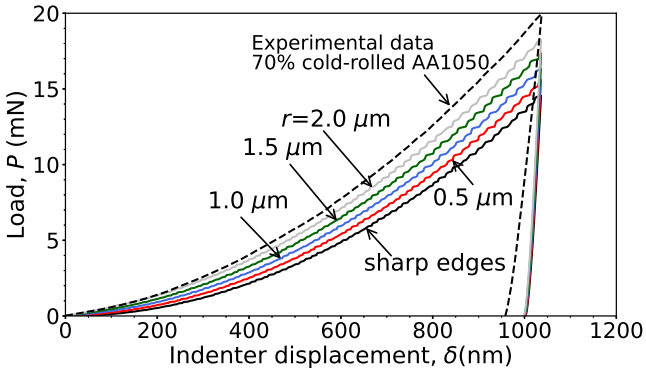

Figure 6. The effect of filler radius, r, on the indentation response using the axisymmetric FE model of Fig. 3 with θ equal to 70.3^o. The friction coefficient, μ, is equal to 0.1. Fig. 4 was used to extract the elastic-plastic behaviour of AA1050.

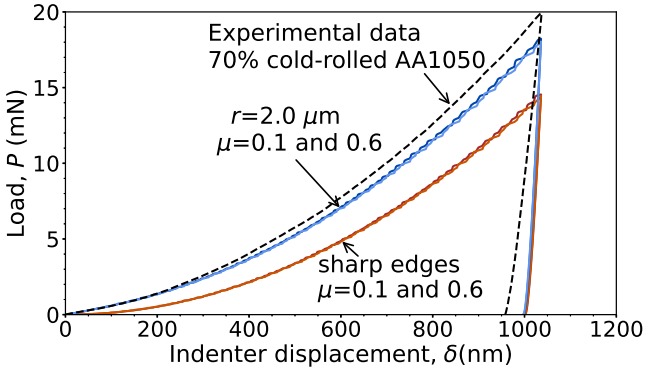

Figure 7. The effect of friction, μ, on the indentation response using the axisymmetric FE model of Fig. 3 with θ equal to 70.3^o. The indenter has sharp edges or a rounded tip with a fillet of radius, r, equal to 2 μm. Fig. 4 was used to extract the elastic-plastic behaviour of AA1050.

of the 70% cold-rolled AA1050 was iteratively modified until a good agreement was found between the numerical predictions and the experimental results. Fig. 8 shows some typical results. It can be seen that when σ_y is equal to 111.2 MPa and n is equal to 0.155, a good agreement is found.

The iterative numerical process showed that other material property combinations showed also a good agreement with the experimentally measured load-displacement curve e.g. for E=63.44 GPa, σ_y=109.24 MPa and n=0.16. Even, when E=60.0 GPa, σ_y=86.83 MPa and n=0.22 the agreement with the experimental response is reasonable. These findings are in agreement with the findings that the elasto-plastic parameters, E, σ_y and n cannot be uniquely obtained from the load displacement curves [7, 11] unless for example two or more indenters with different geometry are used. Here, by assuming that E is the same or close to the Young's modulus of the bulk samples, σ_y and n can be estimated with a certain degree of confidence. However, the procedure presented above has to be repeated in order to verify this claim. At

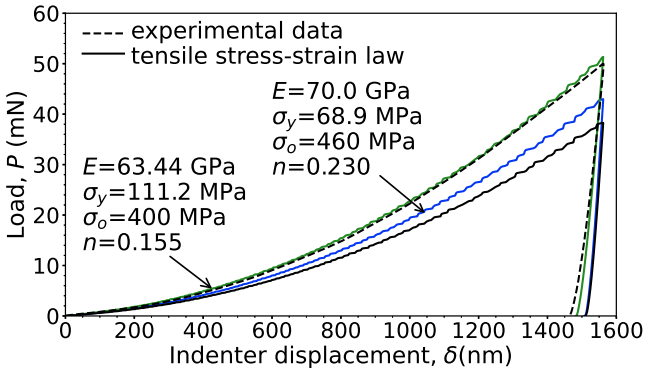

Figure 8. Indentation response using two different stress-strain curves and comparison with the experimentally measured indentation response. The friction coefficient, μ, is equal to 0.1, the filler radius, r, is equal to 2 μm and the indenter angle, θ is equal to 70.3^o.

the same time, the experimental methods to determine the local stresses and strains [12, 13]are also to be further explored, taken into account the internal microstructure and external testing effects.

4. Conclusions

In the present work a numerical iterative approach was presented in order to obtain the elasto-plastic parameters of metals at a small scale from indentation experiments. With a certain degree of confidence, the plastic parameters were estimated. However, using load-displacement curves from the indentation tests using a single indenter geometry does not lead to a unique solution. It is suggested that indenters with different geometries should be used or obtain additional topographic information form the experiments.

Acknowledgements

H. Pan and X. Zhang acknowledges the support from the European Research Council under the European Union Horizon 2020 research and innovation program (grant agreement No 788567-M4D).

References

[1] Zhang X, Hansen N, Gao Y and Huang X 2012 *Acta Materialia* **60** 5933–43
[2] Lu K and Lu J 2004 *Materials Science and Engineering: A* **375-377** 38–45
[3] Dai K and Shaw L 2008 *International Journal of Fatigue* **30** 1398–1408
[4] Hughes D A and Hansen N 2001 *Physical Review Letters* **87**(13) 135503
[5] Rigney D, Naylor M, Divakar R and Ives L 1986 *Materials Science and Engineering* **81** 409–425
[6] Tao N R, Wang Z B, Tong W P, Sui M L, Lu J and Lu K 2002 *Acta Materialia* **50** 4603–16
[7] Tho K K, Swaddiwudhipong S, Liu Z S, Zeng K and Hua J 2004 *Journal of Materials Research* **19** 2498–2502
[8] Giannakopoulos A E and Suresh S 1999 *Scripta Materialia* **40** 1191–98
[9] Zeng K and Chiu C H 2001 *Acta Materialia* **49** 3539–51
[10] Shi Z, Feng X, Huang Y, Xiao J and Hwang K C 2010 *International Journal of Plasticity* **26** 141–8
[11] Cheng Y T and Cheng C M 1999 *Journal of Materials Research* **14** 3493–96
[12] Zhang X, Nielsen C V, Hansen N, Silva C M A and Martins P A F 2019 *International Journal of Plasticity* **115** 93–110
[13] Pan H, He Y and Zhang X 2021 *Materials* **14** 1012